Thermodynamic and Kinetic Studies of the $MgCl_2$-NH_4Cl-NH_3-H_2O System for the Production of High Purity MgO from Calcined Low-Grade Magnesite

Junfeng Wang and Zhibao Li
Key Laboratory of Green Process and Engineering, Institute of Process Engineering, Chinese Academy of Sciences, Beijing 100190, P.R. China

Ah-Hyung Alissa Park
Depts. of Earth & Environmental Engineering and Chemical Engineering, Lenfest Center for Sustainable Energy, Columbia University, New York, NY 10027

Camille Petit
Dept. of Chemical Engineering, Imperial College London, London SW7 2AZ, U.K.

DOI 10.1002/aic.14789
Published online March 27, 2015 in Wiley Online Library (wileyonlinelibrary.com)

To improve the overall sustainability of MgO-based refractory production, a novel process to produce high purity MgO from calcined low-grade magnesite in ammonium chloride solution was developed. The process was designed on the basis of the phase equilibria of the NH_4Cl-$MgCl_2$-NH_3-H_2O system obtained using the Mixed Solvent Electrolyte model embedded in OLI software. The optimum calcination temperature of low-grade magnesite was determined to be 650°C in terms of the conversion ratio of magnesium and calcium in the leaching experiments. An apparent activation energy of Mg extraction was 30.98 kJ/mol, which is slightly lower than that of Ca leaching. An empirical kinetic model of magnesium extraction was also developed to describe the effects of NH_4Cl concentration, particle size of calcined magnesite, and solid-to-liquid ratio on the extent of extraction of magnesium. At leaching time of 10 min, the leachate with high Mg/Ca molar ratio was obtained. Then, MgO with a purity of 99.09% was produced through the decomposition of intermediate $4MgCO_3{\cdot}Mg(OH)_2{\cdot}4H_2O$. © 2015 American Institute of Chemical Engineers *AIChE J*, 61: 1933–1946, 2015

Keywords: kinetic, thermodynamic, solid–liquid reaction, low-grade magnesite, ammonium chloride

Introduction

Magnesite ore is the basic raw material for the manufacturing of MgO-based refractories. The explored magnesite reserves in China amount to about 3×10^{10} tons in the 27 mining areas.[1] About 87% of these resources are located in the Eastern part of Liaoning Province, China. There exist about 30 major producers of light-burned (caustic-calcined) and hard-burned magnesia from high grade magnesite, that is, magnesite with at least 45 wt % of MgO and a low content of silicate and calcium impurities (<2%). It is estimated that the annual production capacities of light-burned magnesia and hard-burned magnesia are about 2.7×10^6 tons and 3.3×10^6 tons, respectively. Unfortunately, low-grade magnesite, that is, magnestite with <44 wt % MgO and a high content of silicate and calcium impurities (>2%), is not fully utilized, which results in a large deposit of mineral tailings (fine powders). This limits the use of magnesite resources and also causes environmental issues. Therefore, an effective method of processing low-grade magnesite has been sought after to produce high value-added products, such as high purity MgO.

Various methods of MgO production from low-grade magnesite have been proposed. Among these methods, the hydrometallurgical method is considered to be most effective in terms of energy and environmental standpoints.[2] Different leaching agents, such as inorganic acids,[3–6] organic acids,[7–12] and inorganic salts[13–16] have been used for the dissolution of magnesium from magnesite or calcined magnesite. When inorganic acids, such as H_2SO_4, HNO_3, or HCl, were used as leaching agents, some undesired impurities, such as Ca, Fe, Si, and Al, were also appreciably dissolved in the leaching process, which caused adverse effects on subsequent handling and affected the quality of the MgO product. Some organic acids were able to selectively extract iron and nickel.[17] However, at high reaction temperatures, organic acids cannot be used as leaching agents because of their low boiling point and decomposition temperature. Thus, inorganic salts, such as calcium chloride or ammonium chloride, have been proposed as an alternative leaching agent to

Additional Supporting Information may be found in the online version of this article.

Correspondence concerning this article should be addressed to A.-H. A. Park at ap2622@columbia.edu or Zhibao Li at zhibaoli@ipe.ac.cn.

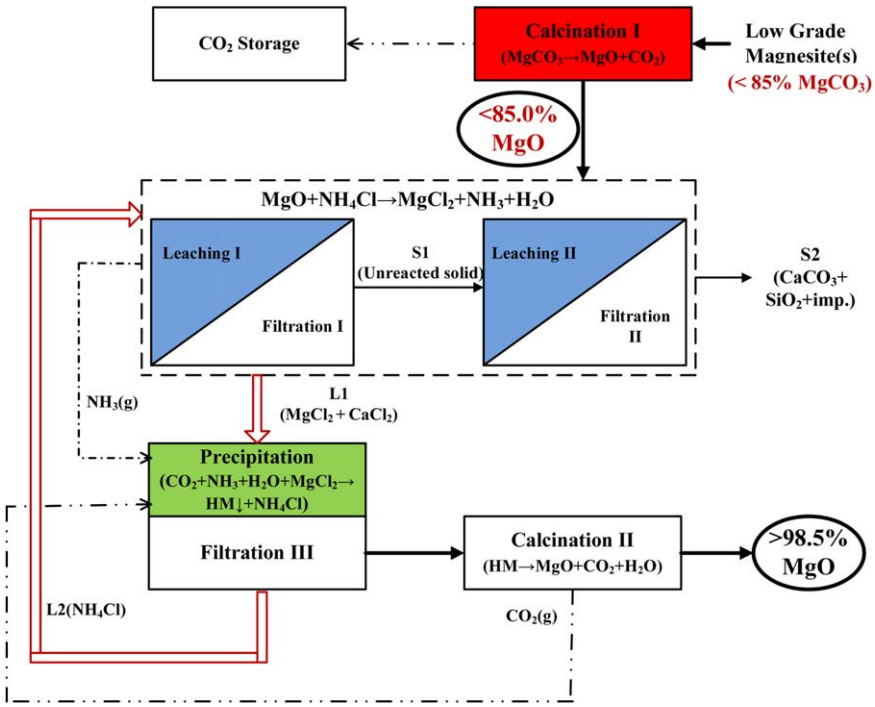

Figure 1. Flow diagram for the production of high purity magnesium oxide from low-grade magnesite (hydromagnesite (HM): $4MgCO_3{\cdot}Mg(OH)_2{\cdot}4H_2O$).

[Color figure can be viewed in the online issue, which is available at wileyonlinelibrary.com.]

selectively dissolve the low-grade magnesite by forming soluble salts.[13]

A chemical process known as SULMAG, has been developed.[18] It is mainly comprised of four steps: (1) leaching of calcined magnesite with calcium chloride and carbon dioxide, (2) precipitation of nesquehonite from the magnesium chloride leachate *via* the introduction of the ammonia and carbon dioxide gases, (3) calcination of $CaCO_3$, and (4) recovery of ammonia from ammonium chloride solution by the Solvay process.[18] The method can produce high quality sintered magnesia from the leachate obtained by dissolving calcined magnesite, and its costs can be minimized by recovering and recycling all the chemical reagents. However, the process of ammonia recovery makes SULMAG complicated. This process involves the reaction of ammonium chloride and lime obtained by the decomposition of $CaCO_3$. Especially, the excess ammonium carbonate must be removed before lime can be added to the ammonium chloride solution, or else the lime will directly combine with carbonate and precipitate as calcium carbonate. Thus, the recovery and recycling of reagents become costly and require a large number of process stages. Ainscow and Gadgil proposed another process, which eliminated the stage of $CaCO_3$ calcination, and supplemented it with a production step of ammonium carbonate.[19]

Inspired by these studies, a relatively simple process of producing high purity MgO from low-grade magnesite using NH_4Cl as leaching agent is investigated in this study. As shown in Figure 1, the proposed method mainly contains three steps: (1) the selective leaching of Mg from calcined low-grade magnesite using NH_4Cl to obtain a leachate with high molar ratio of Mg/Ca, (2) the precipitation of intermediate magnesite carbonate hydrate from the leachate using ammonia and carbon dioxide gases, and (3) production of high purity MgO *via* calcination of intermediate carbonate. The reactions can be summarized as follows

$$MgO(s)+2NH_4Cl(aq) \leftrightarrow MgCl_2(aq)+2NH_3(aq)+H_2O(l) \quad \text{(Rxn. 1)}$$

$$MgCl_2(aq)+NH_3(g)+CO_2(g)+H_2O(l) \leftrightarrow 4MgCO_3 \cdot Mg(OH)_2 \cdot 4H_2O\ (s)+NH_4Cl(aq) \quad \text{(Rxn. 2)}$$

$$4MgCO_3 \cdot Mg(OH)_2 \cdot 4H_2O\ (s) \leftrightarrow 5MgO\ (s)+4CO_2(g)+5H_2O(g) \quad \text{(Rxn. 3)}$$

The reactive crystallization kinetics of $4MgCO_3{\cdot}Mg(OH)_2{\cdot}4H_2O$ in the $MgCl_2$-CO_2-NH_3-H_2O system (Rxn. 2) have been systematically investigated in our previous work.[20] The leaching kinetics of Rxn. 1 is of great importance for understanding the mechanism of the dissolution reaction of calcined magnesite in the $MgCl_2$-NH_4Cl-NH_3-H_2O system. There exist contradictory leaching results of Mg from calcined magnesite. Ranjitham and Khangaonkar[13] observed that the reaction rate was sensitive to reaction temperature, calcination temperature, particle size, and concentration of calcium chloride. It was also found that reaction rate did not depend on either prior hydration or concentration of ammonium chloride (from 2.48 to 5 M). The authors claimed that the leaching rate of magnesium was controlled by a surface chemical reaction with an activation energy of 43.2 kJ/mol. Glaser et al.[15] investigated the leaching kinetics of nonporous pure MgO and porous calcined natural magnesite. Similar to Ranjitham and Khangaonkar, they found that the reacting rate strongly depended on the reaction temperature (from 50°C to 100°C). However, unlike the prior study, they reported that the reaction rate also depended on the ammonium chloride concentration (0.5 $\sim$ 4 M). In addition,

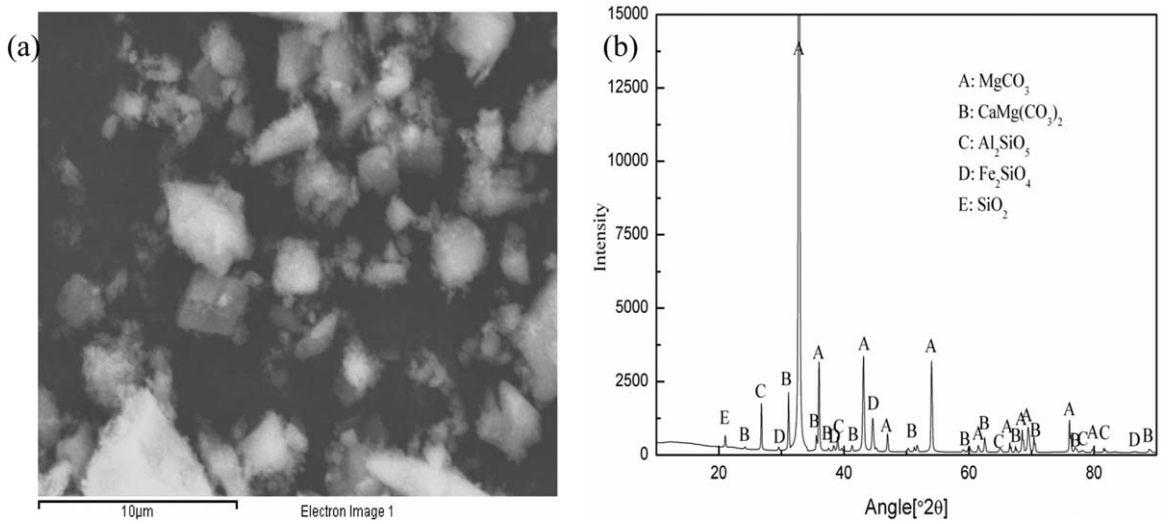

Figure 2. Characterization of low-grade magnesite sample: (a) SEM image and (b) XRD pattern.

they also argued that the leaching rate of magnesium was controlled by the physical dissolution of solid $Mg(OH)_2$ with an apparent activation energy of 39 kJ/mol. To avoid extensive purification steps, in addition to the leaching kinetics, selective dissolution toward Mg is a very important parameter to produce high purity MgO with the content of CaO $<0.5\%$.

The main objective of this study is to obtain the leachate with a high molar ratio of Mg/Ca while using ammonium chloride as a leaching agent promoting the selective dissolution of magnesium from the calcined low-grade magnesite. Rigorous thermodynamic and kinetic models of the NH_4Cl-$MgCl_2$-NH_3-H_2O system are also established to analyze the phase and reaction behaviors of reactants and intermediates.

Material and Experimental

Materials

Ammonium chloride with a purity of 99.0% was supplied by Beijing Chemical Reagent and was used without further purification. A series of NH_4Cl solutions were prepared by dissolving NH_4Cl in deionized water (conductivity <0.1 μS/cm). Their concentrations ranged from 2 to 6 M with an interval of 2 M.

The representative sample of low-grade magnesite was kindly donated by the Zhongmei Magnesium Products, Haicheng, China. The natural magnesite was crushed, ground, and calcined at a given temperature for 4 h. After calcination, the weight of each sample was measured to obtain the weight loss. Calcined magnesite samples were sieved using ASTM standard sieves ($-0.25+0.10$, $-0.40+0.25$, $-0.50+0.40$, and $-0.80+0.50$ mm).

Particle characterization

Scanning electron microscopy (SEM, JEOL JSM–7001F), coupled with energy-dispersive X-ray spectroscopy (EDS, Oxford INCA 250) were used to characterize the natural magnesite, and the SEM image is shown in Figure 2a. The X-ray diffraction (XRD) pattern of the natural magnesite was also obtained (Siemens D5000 X-ray diffractometer with CuKα radiation), as shown in Figure 2b. The results indicate that the natural magnesite contained essentially $MgCO_3$ and $CaMg(CO_3)_2$. The results of chemical analysis performed using ICP-OES (PE Optima 5300DV, PerkinElmer) are reported in Table 1. It was found that natural magnesite contained 41.95% of MgO, which was significantly lower than the theoretical MgO content of pure magnesite (47.82%). In addition, the sample contained SiO_2 of 4.91%, CaO of 1.92% and other impurities, confirming that the studied magnesite samples were of low-grade ore.

Experimental procedure for leaching kinetics

Here, the calcination temperature of low-grade magnesite ranged from 600°C to 850°C, the initial NH_4Cl concentration from 2 to 6 mol/L with an interval of 2 mol/L, the reaction temperature from 50°C to 100°C, the reaction time from 0 to 180 min, the solid-to-liquid ratio from 20/500 to 40/500 g/mL with an interval of 10/500 g/mL, and the particle size from $-0.25+0.10$ to $-0.80+0.50$ mm.

The procedure of the experiments was as follows: 500 mL of the prepared NH_4Cl solution was added to a 1000 mL jacketed glass reactor equipped with a water-cooled condenser to minimize solution losses due to evaporation. A propeller agitator inside the glass reactor provided internal circulation of the suspension. The stirring speed was kept at 400 rpm during the experiments to satisfy hydrodynamic requirements, maintain stable mixing and avoid external mass transfer limitation (a test at 300 rpm ruled out external mass transfer limitation). The temperature of the solution in the reactor was kept constant using a circulating oil batch equipped with a thermoelectric controller. When the desired operating temperature was reached, a weighted mineral sample was added to the reactor, and the solution pH was measured using a pH-thermometer.

To collect the kinetic data on the dissolution of Mg and Ca from the calcined low-grade ore, slurry samples were collected from the reactor at predetermined time intervals. It

Table 1. Results of Chemical Analysis of the Low-Grade Magnesite Sample

Component	MgO	CaO	SiO_2	Al_2O_3	Fe_2O_3	L.O.I
Content (wt %)	41.95	1.92	4.91	0.86	0.56	49.80

was then immediately filtered using a 0.2 μm filter membrane to stop any further reactions. The clear filtrate was used to measure the concentrations of Mg^{2+} and Ca^{2+} ions. The magnesium content was determined by complexometric titration with EDTA at pH 9.5–10 (ammonia buffer) using Eriochrome black T as the indicator. The Ca^{2+} content in the liquid sample was determined by titration with EDTA and tetracarboxylate as indicators. The extent of Mg and Ca dissolution were then calculated using the following expression

$$X_A = \frac{VC_A}{Wx_A} \times MW_A \quad (1)$$

where C_A is the concentration of Mg^{2+} or Ca^{2+} in the liquid phase (mol/L), V is the volume of the leaching aqueous solution (L), W is the weight of the added sample (g), x_A is the element content of Mg or Ca in the added sample, and $MW_A$is the molecular weight of Mg^{2+} or Ca^{2+}.

Experiment procedure with distillation of the ammonia

To increase the extent of Mg dissolution, leaching experiment of calcined low-grade magnesite by distillation of the ammonia was carried out. The apparatus consisted of a reboiler flask with a volume of 2 L, a condenser with decanter at the bottom, and a heating jacket with maximum heating power of 0.5 kW. The condenser was cooled using tap water. The procedure of the experiments was as follows: 1000 mL of the prepared NH_4Cl solution and 60 g sample was first added to the flask. Then, the flask was slowly heated to the boiling point temperature. The temperature of the flask is around 106°C, which is almost 8.5°C higher than that of the overhead vapor. The vapor was condensed and returned back to the flask. Ammonia released from the top of the condenser was absorbed using the HCl solution. Once ammonia emissions from the leaching liquor ceased, the reaction was stopped. The concentrations of Mg^{2+} and Ca^{2+} ions in the solution were measured according to the above section.

Thermodynamic and Kinetic Models

Leaching process fundamental theory

Ammonium chloride is a salt formed between a strong acid and a weak base and it ionizes in an aqueous medium

$$NH_4Cl \leftrightarrow NH_4^+ + Cl^- \qquad (\log(K_1) = 1.24 \text{ at } 25°C) \quad \text{(Rxn. 4)}$$

Subsequently, ammonium ions react with water to form ammonia and hydronium ions

$$NH_4^+(aq) + H_2O(l) \leftrightarrow NH_3(aq) + H_3O^+(aq) \qquad (\log(K_2) = -9.24 \text{ at } 25°C) \quad \text{(Rxn. 5)}$$

When MgO is added to the NH_4Cl solution, H_3O^+ derived from the hydrolysis of NH_4^+ (Rxn. 5) can enhance the dissolution of MgO forming additional Mg^{2+}. While this pH effect is not as significant as the cases with strong acid (e.g., HCl and HNO_3), the use of NH_4Cl is attractive due to its potential recovery *via* NH_3(g) recycle. The overall reaction of MgO dissolution in NH_4Cl solution can be written as followed

$$MgO(s) + 2NH_4Cl(l) \leftrightarrow Mg^{2+}(aq) + 2NH_3(g) + H_3O(l) + 2Cl^-(aq) \quad \text{(Rxn. 6)}$$

The equilibrium in Rxn. 6 lies far to the right, toward the production of NH_3. Therefore, the reaction can be considered as an irreversible reaction owing to the effective removal of NH_3(g) produced during the MgO leaching process *via* stirring or increasing the reactor temperature of the reaction mixture. To systematically analyze the phase behavior of the leach liquor, a new thermodynamic model of phase equilibria for the $MgCl_2$-NH_4Cl-NH_3-H_2O system is indispensable and was established based on the Mixed Solvent Electrolyte (MSE) model (available as software package Stream-Analyzer 3.2) embedded in OLI platform.[21]

MSE model

The thermodynamic equilibrium constant, K, can be calculated using the following equation

$$K = \exp\left(-\frac{\Delta_R \bar{G}^0}{RT}\right) \quad (2)$$

where $\Delta_R \bar{G}^0$ is the partial molar, standard-state Gibbs free energy of the reaction (kJ·mol^{-1}), R is the universal gas constant (8.314 J·mol^{-1}·K^{-1}), and T is the temperature (K). To obtain the equilibrium constant (K), the standard-state chemical potentials of the products and reactants must be known. For solids, the standard-state chemical potentials were calculated using the standard-state Gibbs free energy of formation ($\Delta_f G^0$), entropy (S^0), and heat capacity (C_p^0). For aqueous species, the HKF model developed by Tanger and Helgeson[22] was used. Thermodynamic data of equilibrium species at standard-state were taken from the databank of the MSE model embedded in OLI platform.[21]

While thermodynamic equilibrium constants are generally used to calculate the chemical equilibriums, the nonideality of an electrolyte solution can be represented by the excess Gibbs free energy. In the MSE model, the excess Gibbs free energy, G^{ex}, is constructed as following[21]

$$\frac{G^{ex}}{RT} = \frac{G^{ex}_{LR}}{RT} + \frac{G^{ex}_{MR}}{RT} + \frac{G^{ex}_{SR}}{RT} \quad (3)$$

where G^{ex}_{LR} represents the contribution of long-range electrostatic interactions expressed by the Piter-Debye–Hückel equation, G^{ex}_{SR} is the short-range contribution resulting from molecule–molecule, molecule–ion, and ion–ion interactions calculated by the UNIQUAC model, and an additional middle-range term G^{ex}_{MR} accounts for ionic interactions that are not included in the long-range term. G^{ex}_{MR} is calculated from a symmetrical second-virial coefficient-type expression[21]

$$\frac{G^{ex}_{MR}}{RT} = -\left(\sum_i n_i\right)\sum_i\sum_j x_i x_j B_{ij}(I_x) \quad (4)$$

where x is the mole fraction of the species, I_x represents the ionic strength, and B_{ij} is a binary interaction parameter between the species i and j (ion or molecule; i.e., $B_{ij}(I_x)=B_{ji}(I_x)$, $B_{ii}(I_x)=B_{jj}(I_x)=0$). B_{ij} is a function of ionic strength represented by the following empirical expression[20]

$$B_{ij}(I_x) = b_{ij} + c_{ij}\exp\left(-\sqrt{I_x + 0.01}\right) \quad (5)$$

where b_{ij} and c_{ij} are adjustable parameters. In general, the parameters b_{ij} and c_{ij} are obtained as a function of temperature as[21]

$$b_{ij}=\mathrm{BMD0}+\mathrm{BMD1}\times T+\mathrm{BMD2}/T+\mathrm{BMD3}\times T^2+\mathrm{BMD4}\times \ln T \tag{6}$$

$$c_{ij}=\mathrm{CMD0}+\mathrm{CMD1}\times T+\mathrm{CMD2}/T+\mathrm{CMD3}\times T^2+\mathrm{CMD4}\times \ln T \tag{7}$$

where BMD and CMD# are the interaction parameters.

In practice, the middle-range parameters are used to account for ion–ion and ion–neutral molecule interactions, and the short-range parameters are used to represent neutral–neutral interactions.[21] Therefore, the middle-range parameters were mainly considered in this work because these were most important for the systems of interest.

Leaching kinetic models

For most oxide minerals, the hydrometallurgical leaching process is, in general, controlled by the chemical surface reaction and followed by diffusion through the fluid film and/or inert ash layer of the reactant.[23] The leaching of calcined low-grade magnesite in NH_4Cl-H_2O system would proceed *via* the following steps (The bulk diffusion of reactant and product was assumed to be very fast due to rapid mixing as well as Rxns. 5 and 6).

1. Mass transfer of H^+ in the fluid boundary layer to the outer surface of the calcined magnesite particle,
2. Diffusion of H^+ through the inert ash layer adjacent to the surface of the unreacted calcined magnesite,
3. Heterogeneous surface reaction between H^+ and the calcined magnesite particle,
4. Diffusion of the product (Mg^{2+} or Ca^{2+}) through the inert ash layer back to the surface of the outer calcined magnesite particle and,
5. Diffusion of the product (Mg^{2+} or Ca^{2+}) through the fluid boundary layer back into the bulk fluid.

Thus, Steps 1–3 were considered as a potential rate-limiting steps.[23] To determine the kinetic parameters and the rate-limiting step of the leaching of calcined low-grade magnesite in NH_4Cl solutions, the experimental data was analyzed on the basis of the shrinking core model.[24–27] In this model, the dissolution reaction initially takes place on the outer skin of the calcined magnesite particle. However, as the reaction proceeds, the reactive surface of the reaction is progressively shifted into the interior of the solid to leave behind an inert ash layer (e.g., Si-rich layer). To reach the surface of the unreacted core, H^+ must travel through various layers of resistances, as described above.

Steps 1–3 of the dissolution of calcined low-grade magnesite can be modeled as following. The mass transfer rate (W_1) of H^+ in the fluid boundary layer to the outer surface of calcined magnesite particle is

$$W_1 = 4\pi r_0^2 k_l (C_\mathrm{b}-C_\mathrm{s}) \tag{8}$$

where C_b and C_s are the concentrations of H^+ in the bulk fluid and at the external surface of the particle, respectively. The mass transfer coefficient, k_l, is the function of the radius of particle, r_0.

The diffusion rate (W_2) of H^+ through the inert ash layer to the inner surface of the unreacted particle is

$$W_2 = 4\pi r_t^2 D_\mathrm{eff}\frac{dC}{dr} \tag{9}$$

where D_eff is the effective diffusion coefficient. From this relationship, one can derive the following equation

$$W_2 = 4\pi D_\mathrm{eff}\frac{C_\mathrm{s}-C_\mathrm{c}}{1/r_\mathrm{c}-1/r_0} \tag{10}$$

with the boundary conditions

$$C=\begin{cases} C_\mathrm{s} & \text{at} \quad r=r_0 \\ C_\mathrm{c} & \text{at} \quad r=r_\mathrm{c} \end{cases} \tag{11}$$

Here, C_c is the concentration of H^+ at the surface of the unreacted core. The rate of consumption, W_3, of H^+ at the reactive surface of unreacted core is

$$W_3 = 4\pi r_\mathrm{c}^2 k_\mathrm{r} C_\mathrm{c} \tag{12}$$

where k_r is the reaction rate constant. Under pseudo-steady-state conditions, the mass transfer rate of H^+ in the fluid boundary layer and the diffusion rate of H^+ through the inert ash layer are equal to the rate of consumption of H^+ at the surface of the unreacted core. Hence

$$R_\mathrm{s}=W_3 = -W_1=-W_2 \tag{13}$$

Substituting Eqs. 8, 10, and 12 into Eq. 13, $C_\mathrm{c}$and C_s can be eliminated, and the main reaction rate, R_s, is obtained

$$R_\mathrm{s}=-\frac{4\pi r_0^2 C_\mathrm{b}}{1/k_\mathrm{l}+(1/k_\mathrm{r})(r_0/r_\mathrm{c})^2+(r_0(r_0-r_\mathrm{c}))(D_\mathrm{eff}r_\mathrm{c})} \tag{14}$$

In addition, the dissolution rate of the particle can be expressed in term of the reduction rate of the size of the unreacted core

$$R_\mathrm{s} = \frac{d}{dt}\left(\frac{4}{3}\pi r_\mathrm{c}^3\rho_\mathrm{s}/M\right) \tag{15}$$

where t is the leaching time, M is the molar weight of particle, and ρ_s is the particle density. Thus, the conversion of the mineral dissolution is related to the radius of the particle *via* the following equation

$$X_\mathrm{A} = 1-\left(\frac{r_\mathrm{c}}{r_0}\right)^3 \tag{16}$$

From Eqs. 14–16, the conversion as a function of time, ${dX_\mathrm{A}}/{dt}$, is

$$\frac{dX_\mathrm{A}}{dt} = \frac{3MC_\mathrm{b}}{\rho_\mathrm{s}r_0\left[1/k_\mathrm{l}+(1/k_\mathrm{r})(1-X_\mathrm{A})^{-2/3}+(r_0/D_\mathrm{eff})((1-X_\mathrm{A})^{-1/3}-1\right]} \tag{17}$$

By integrating Eq. 17, the basic equation for the unreacted shrinking core model used to describe the leaching kinetic of calcined magnesite particle can be obtained as follows[26]

$$\frac{X_\mathrm{A}}{3k_\mathrm{l}}+\frac{r_0}{6D_\mathrm{eff}}\left[1-3(1-X_\mathrm{A})^{2/3}+2(1-X_\mathrm{A})\right]+\frac{1}{k_\mathrm{r}}\left[1-(1-X_\mathrm{A})^{1/3}\right]=\frac{MC_\mathrm{b}}{\rho_\mathrm{s}r_0}t \tag{18}$$

Based on the above equation, different empirical kinetic equations can be obtained. If the leaching process is controlled by the fluid film diffusion, the integrated kinetic equation becomes

$$k_\mathrm{l}t=X_\mathrm{A}=\frac{3Mk_\mathrm{l}C_\mathrm{b}}{\rho_\mathrm{s}r_0}t \tag{19}$$

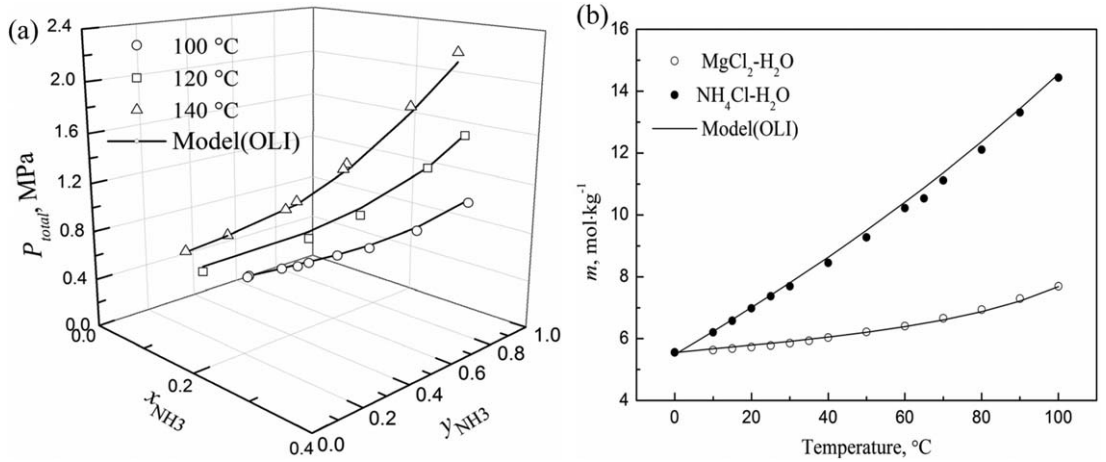

Figure 3. (a) Experimental (points) and calculated (lines) mole fractions of NH_3 in both liquid and gas phases, and total pressure for the binary NH_3-H_2O system at various temperatures. (b) Experimental (points) and calculated (lines) solubilities of $MgCl_2$ and NH_4Cl in water at various temperatures.

If the leaching process is controlled by the inert ash layer diffusion, the integrated kinetic equation becomes

$$k_2 t = 1 - 3(1 - X_A)^{2/3} + 2(1 - X_A) = \frac{6MD_{eff}C_b}{\rho_s r_0^2} t \qquad (20)$$

If the leaching process is controlled by the surface chemical reaction, then the integrated kinetic equation is as follows

$$k_3 t = 1 - (1 - X_A)^{1/3} = \frac{Mk_r C_b}{\rho_s r_0} t \qquad (21)$$

where k_1, k_2, and k_3 are the reaction rate constants. The rate-limiting step and kinetic mechanism for the leaching of calcined magnesite in NH_4Cl solutions were determined by applying these kinetic equations to the experimental data obtained in this study.

Results and Discussion

Calculation of new MSE parameters for thermodynamic model

The accuracy of the existing MSE model parameters in estimating phase equilibria data of the systems relevant to this study was first evaluated by comparing predictions based on OLI parameters to literature experimental data (See Supporting Information Table S1, column *ARD*). For the binary NH_3-H_2O system, the solubility of NH_3 as well as its vapor–liquid equilibria over the pressure range from 0 to 3.2 MPa was evaluated over the temperature range from 100°C to 140°C.[28,29] The results were compared to literature values as shown in Figure 3a. The calculated results were quite consistent with the experimental values with an overall average relative deviation (ARD) of 2.55%. For the binary NH_4Cl-H_2O and $MgCl_2$-H_2O systems, the model's prediction based on OLI parameters and the experimental data taken from literature[30,31] were compared over the temperature range from 0°C to 100°C. As shown in Figure 3b, the existing model again gave a good result for the solubility of NH_4Cl and $MgCl_2 \cdot 6H_2O$ in water with the overall ARDs of 1.49% and 0.71%, respectively.

Conversely, for the ternary NH_4Cl-NH_3-H_2O and NH_4Cl-$MgCl_2$-H_2O systems as well as the quaternary NH_4Cl-$MgCl_2$-NH_3-H_2O system, significant deviations between calculated values and experimental data were observed with overall ARDs of 5.57%, 15.12%, and 48.26%, respectively (dotted lines in Figures 4a, b and 5). Therefore, in this study, a new set of MSE parameters for these three systems were obtained by fitting various literature values. The new MSE model parameters for NH_3-NH_4^+ and $NH_4^+ - Mg^{2+}$ were determined *via* the linear regression of phase equilibrium data for the two NH_4Cl-NH_3-H_2O and NH_4Cl-$MgCl_2$-H_2O systems found in various literature. In this regression, the model parameters listed in Supporting Information Table S2 were obtained by minimizing the sum of squared deviations between the experimental and calculated values of solubility. Using the new MSE model parameters, the phase equilibria of the NH_4Cl-NH_3-H_2O and NH_4Cl-$MgCl_2$-H_2O systems was recalculated. As it can be seen from Figures 4a, b (solid lines), the calculated results were in good agreement with the experimental values with overall ARD of 1.27% and 1.62% for NH_4Cl-NH_3-H_2O and NH_4Cl-$MgCl_2$-H_2O systems, respectively.

In case of the NH_4Cl-$MgCl_2$-NH_3-H_2O system, only limited experimental data were available in literature covering a very narrow temperature range of 10–29°C.[29] Regardless, the recalcualted results were in good agreement with the experimental values as shown in Figure 5 (solid line). Thus, it was confirmed that the new set of MSE model parameters are better at calculating phase equilibria of ternary and quaternary systems involving NH_4Cl and $MgCl_2$.

Optimization of reaction parameters for high Mg to Ca ratio

The leaching behavior of Mg and Ca from calcined magnesite using NH_4Cl was investigated to tune the Mg/Ca molar ratio. Here, the goal was to maximize the leaching selectivity toward Mg to avoid the need for additional purification steps. A number of reaction variables influencing the Mg leaching including the calcination temperature of low-grade magnesite, the initial NH_4Cl concentration, the reaction temperature, the reaction time, the solid-to-liquid ratio, and the particle size were investigated.

Effect of Calcination Temperature. The influence of the calcination temperature (600–850°C) on phase composition and crystallinity of calcined magnesite was studied. As

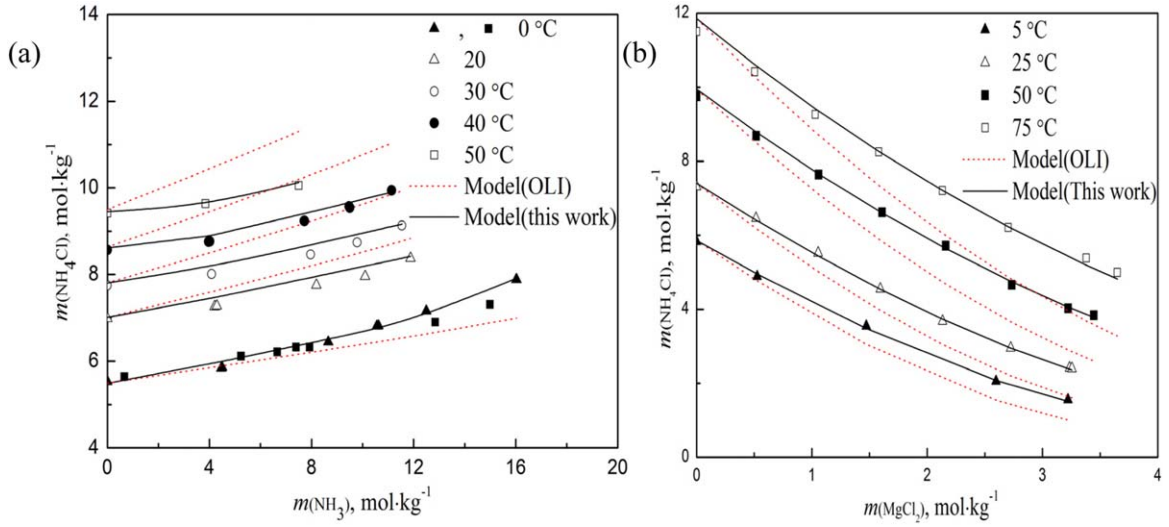

Figure 4. Experimental (points) and calculated (solid and dotted lines) solubilities of NH_4Cl at various temperatures in two different systems: (a) NH_4Cl-NH_3-H_2O and (b) NH_4Cl-$MgCl_2$-H_2O.

[Color figure can be viewed in the online issue, which is available at wileyonlinelibrary.com.]

shown in Figure 6a, starting from 600°C, the main phases of the starting (i.e., $MgCO_3$ and $CaMg(CO_3)_2$) progressively disappeared. The unconverted $MgCO_3$ content was reduced from 10.58% at 600°C, 1.74% at 650°C, and to 1.47% at 700°C. At a calcination temperature of 750°C and beyond, these minerals were completely disappeared and the structure of calcined magnesite appeared to be highly ordered. At calcination temperature of 850°C, a minor new phase, CaO, was formed. The EDS analysis of calcined magnesite sample shown in Figure 6b indicates that SiO_2 and $CaCO_3$ were randomly dispersed in the MgO phase.

The calcination temperature dependence on the extent of Mg and Ca leaching was investigated under the following dissolution conditions: initial NH_4Cl concentration of 4 M, reaction temperature of 70°C, solid-to-liquid ratio of 60 g/L, particle size fraction of $-0.50 + 0.40$ mm, and stirring speed of 400 rpm. The pH value of initial ammonium chloride solution was 3.76, and increased to about 7.40 $\sim$ 7.80 at the end of the leaching experiment. During each leaching process, ammonia and magnesium chloride buffered systems were formed in the reaction medium, and the leaching products (i.e., $MgCl_2$ and $CaCl_2$) were soluble in the reaction medium.

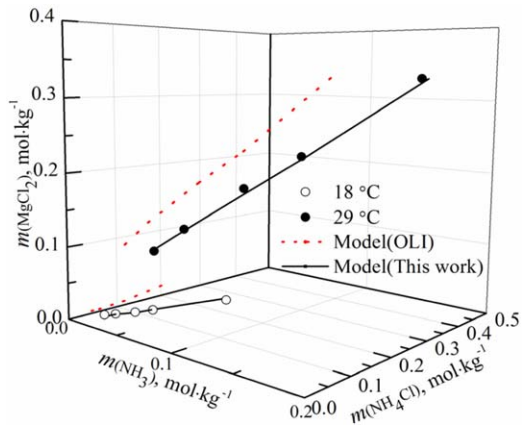

Figure 5. Experimental (points) and calculated (lines) solubilities of $MgCl_2$ in the quaternary system NH_4Cl-$MgCl_2$-NH_3-H_2O at 18°C and 29°C.

[Color figure can be viewed in the online issue, which is available at wileyonlinelibrary.com.]

The extent of Mg dissolution as a function of leaching time was obtained for samples calcined at different calcination temperatures and the results are shown in Figure 7a. In all cases, the initial dissolution rate of Mg was very fast, but the conversion, in terms of Mg leaching, X_{Mg}, was leveled off at different values after 10 min of leaching time (43.51%, 49.42%, 55.53%, 57.63%, and 46.03% for samples calcined at 850°C, 750°C, 700°C, 650°C, and 600°C, respectively). After 20 min of reaction, almost no additional Mg was released from the calcined magnesite. Over the calcination temperatures ranging from 850°C to 700°C, lower calcination temperatures led to increasing Mg concentrations in the leach liquor. This may be due to the formation of periclase (a cubic form of MgO) which has been reported at calcination temperatures >700°C.[14] A further decrease in calcination temperature to 650°C did not make a notable change in the Mg leaching. However, calcination temperature of 600°C was found to be unfavorable for the dissolution of Mg from calcined magnesite. This result indicates that 600°C is insufficient to completely decompose $MgCO_3$ into MgO. As shown in Figure 6a, the sample calcined at 600°C still exhibited a high carbonate content compared to other samples.

To investigate the selectivity of the Mg leaching, Ca concentration in each leach liquor sample was also measured. As shown in Figure 7b, the increase in the calcination temperature resulted in greater Ca leaching. But more importantly, the Mg/Ca molar ratios at the reaction time of 10 min were found to be: 387, 405, 388, 58, and 12 for the samples calcined at 600°C, 650°C, 700°C, 750°C, and 850°C, respectively. Therefore, for the subsequent experiments, the calcination temperature of 650°C was selected as it corresponded to the best condition for high Mg leaching and high Mg purity.

Effect of Leaching Temperature. To study the effects of the reaction temperature on the leaching rates of Mg and Ca,

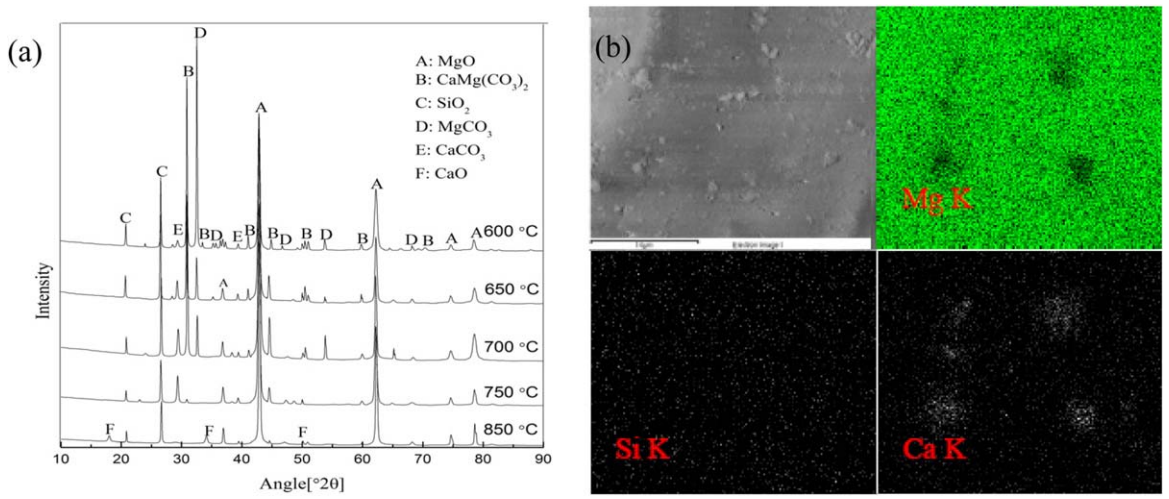

Figure 6. Characterization of the calcined low-grade magnesite: (a) XRD patterns and (b) EDS mapping.

[Color figure can be viewed in the online issue, which is available at wileyonlinelibrary.com.]

the solution temperature was varied from 50°C to 100°C. Initial NH_4Cl concentration, particle size, solid-to-liquid ratio, and stirring speed were kept constant at 4 M, $-0.50 + 0.40$ mm, 60 g/L, and 400 rpm, respectively. As shown in Figure 8a-1, the experimental results indicated that an increase in reaction temperature had a positive effect on the leaching process. A higher leaching rate for Mg was observed within the first 10 min of the reaction for all cases before leveling off. The limited extraction of Mg may be attributed to two main factors: the formation of diffusion-limiting phases during the leaching process and a pH change *via* degassing of NH_3. As mentioned previously, NH_4Cl behaved similarly to HCl and HNO_3. The initial reaction rate would be dominated by the surface reaction rate but then quickly limited by the ash layer diffusion. Thus, the reaction rates were leveled off. In contrast to the extent of Mg leaching, an increase of reaction temperature had a negative effect on the molar ratio of Mg/Ca (Figure 8a-2). This trend was particularly pronounced at reaction temperature above 70°C. The Mg/Ca molar ratios at the leaching time of 10 min were: 410 at 50°C, 405 at 70°C, 314 at 90°C, and 260 at 100°C. Thus, an optimization between the conversion and the purity of Mg should be considered as a function of reaction temperature. In this study, the reaction temperature of 70°C, which resulted in high Mg leaching conversion and high Mg/Ca ratio, was selected for the subsequent experimental studies.

Effect of NH_4Cl Concentration. To investigate the effects of NH_4Cl concentration on the conversion ratio of Mg and Ca leaching, the experiments were carried out in the 2–6 M NH_4Cl solution. Other parameters were kept constant: reaction temperature of 70°C, particle size of $-0.50 + 0.40$ mm, stirring speed of 400 rpm, and solid-to-liquid ratio of 60 g/L. As shown in Figure 8b-1, a higher initial solution concentration resulted in a higher conversion in term of Mg leaching from calcined magnesite. At the leaching time of 10 min, the extent of Mg extraction reached: 67%, 58%, and 47% in 6 M, 4 M, and 2 M NH_4Cl solutions, respectively. The molar ratio of Mg/Ca for each leach liquor sample shown in Figure 8b-2 illustrated that the extraction of Ca was easier than that of Mg. Thus, as the NH_4Cl concentration decreased from 4 to 2 M, the purity of Mg-bearing product was lowered significantly. Conversely, the increase in NH_4Cl concentration from 4 to 6 M did not impact the molar ratio of

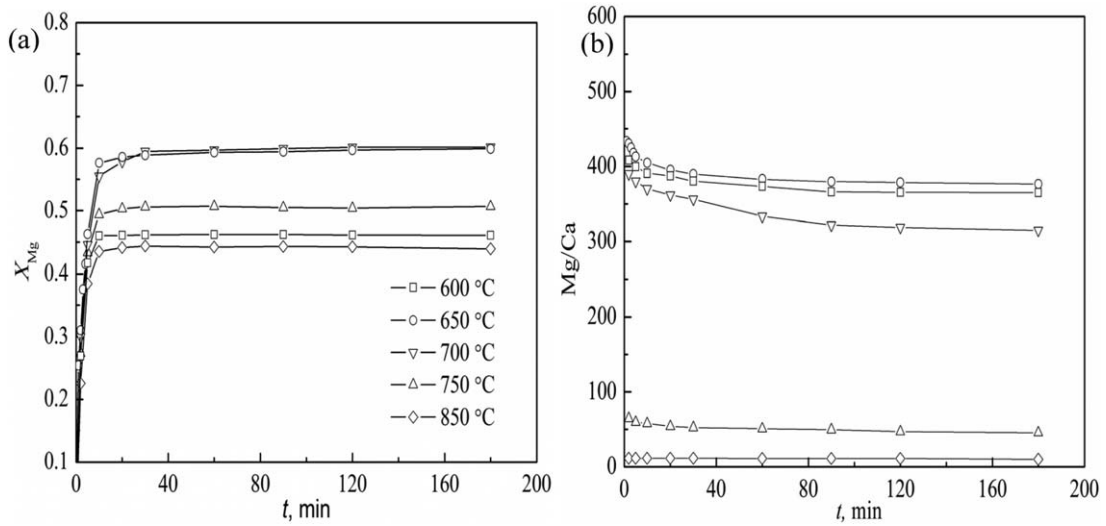

Figure 7. Effect of calcination temperature on: (a) the extent of Mg dissolution and (b) the Mg/Ca molar ratio.

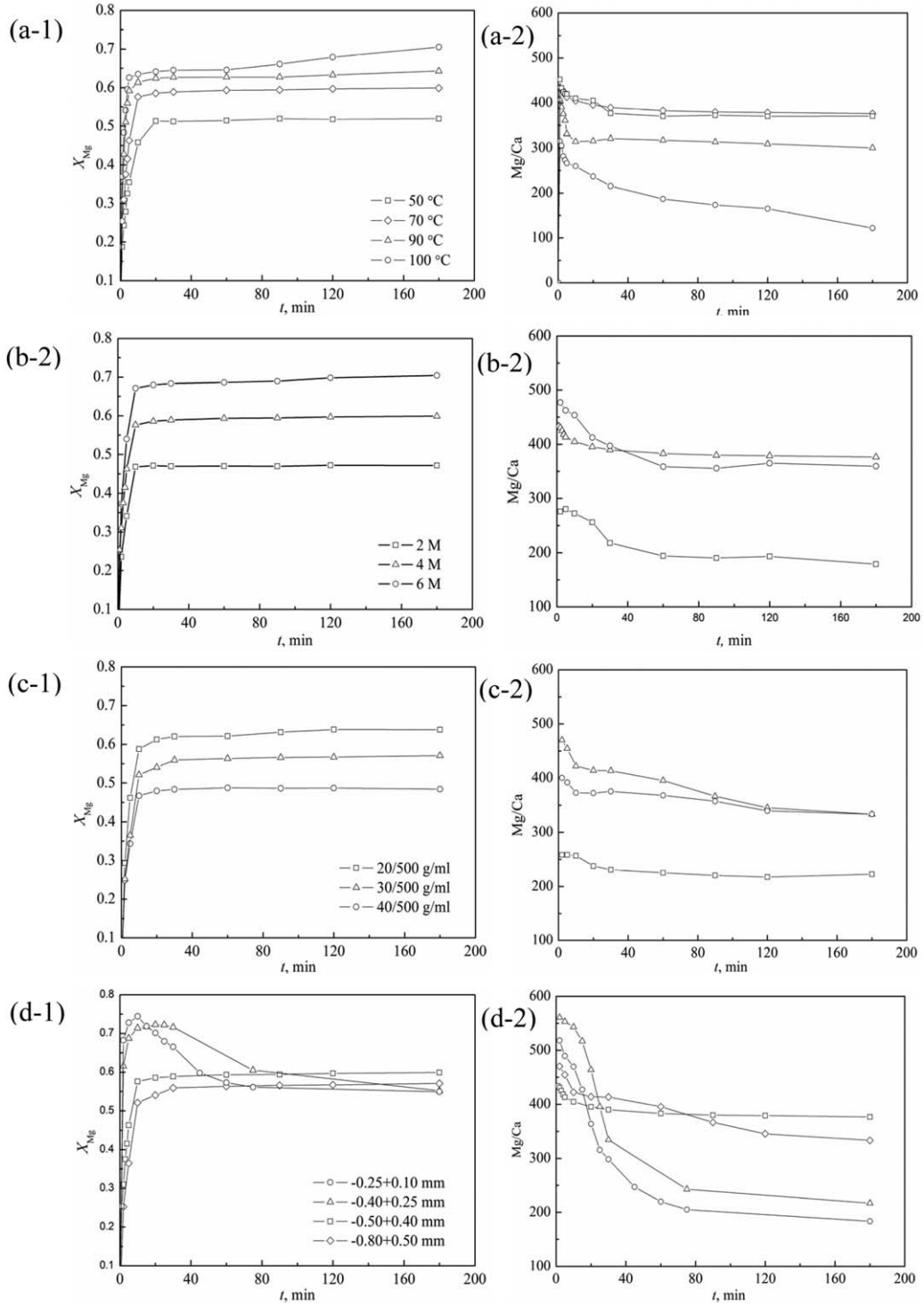

Figure 8. Effect of leaching temperature, NH_4Cl concentration, solid-to-liquid ratio, and particle size on: (a-1, b-1, c-1, d-1) the extent of Mg dissolution and (a-2, b-2, c-2, d-2) the Mg/Ca molar ratio.

Mg/Ca. The results indicate that the leachate with higher Mg/Ca molar ratio could not be achieved by simply increasing the concentration of NH_4Cl.

Effect of Solid-to-Liquid Ratio. The effects of the solid-to-liquid ratio on the extent of Mg extraction and the Mg/Ca mole ratio were determined in the range of 40–80 g/L solid-to-liquid ratios. In these experiments, NH_4Cl concentration, particle size, stirring speed, and reaction temperature were kept constant at 4 M, $-0.80 + 0.50$ mm, 400 rpm, and 70°C, respectively. An increase in the solid-to-liquid ratio caused a decrease in the conversion of Mg leaching (Figure 8c-1). This indicates that the reaction was limited by the solvent, rather than calcined magnesite. In addition, the Mg/Ca molar ratio initially increased and then decreased with increasing solid-to-liquid ratio (Figure 8c-2), but eventually, leveling off at the same value for 60–80 g/L cases. In other words, 60–80 g/L of solid-to-liquid ratios would be optimal for the Mg extraction from calcined magnesite.

Effect of Particle Size. The effect of the particle size on the dissolution rate of Mg and Ca were studied using the

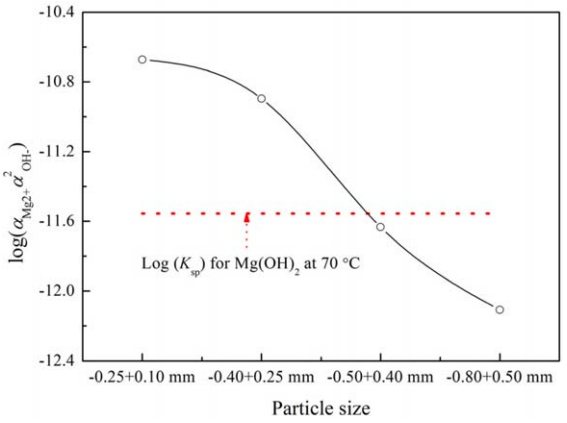

Figure 9. Ionic activity product for different particle size at 70°C.

[Color figure can be viewed in the online issue, which is available at wileyonlinelibrary.com.]

following size fractions: $-0.25+0.10$, $-0.40+0.25$, $-0.50+0.40$, and $-0.80+0.50$ mm. The NH_4Cl concentration, solid-to-liquid ratio, stirring speed, and reaction temperature were kept constant of 4.00 M, 60 g/L, 400 rpm, and 70°C, respectively. As shown in Figure 8d-1, there was an initial sharp increase in Mg concentration in the leach liquor for all cases, while as expected the effect was more pronounced for smaller particles, which possessed higher surface area-to-volume ratio. As shown in Figure 8d-1, what came after the initial dissolution phase was more interesting. In the case of two smallest particle cuts ($-0.25+0.10$ and $-0.40+0.25$ mm), the Mg concentration in the leaching solvent actually decreased and converged to the same level as all other cases. This may be due to the subsequent formation of $Mg(OH)_2$ in the system. This phenomenon was only observed in these two cases because the dissolution kinetics of very fine particles are known to be orders of magnitude greater than that of larger particles due to the presence of highly disordered surfaces.[32] The initial spike in the Mg concentration must have taken place faster than the degassing of NH_3. Thus, the formation of $Mg(OH)_2$ became evident, and thus, the apparent concentration of Mg in the liquid phase was dropped.

This phenomenon was also explained by the equilibrium pH values of the NH_4Cl-$MgCl_2$-NH_3-H_2O system (i.e., 7.40 for $-0.25+0.10$ mm and 7.42 for $-0.40+0.25$ mm), which were calculated using the new MSE parameters. These pH values were lower than those measured at the leaching time of 10 min: 8.20 and 8.09 for $-0.25+0.10$ and $-0.40+0.25$ mm, respectively. With the relatively slower removal rate of NH_3 compared to the buildup of Mg concentration in the liquid phase, NH_3 in the solution phase led to the formation of hydroxide ions (Rxn. 7), which was promoted by the subsequent reaction consuming OH^- (Rxn. 8)

$$NH_3+H_2O \leftrightarrow NH_4^+ + OH^- \quad (\log(K_3)=-4.76 \text{ at } 25°C) \tag{Rxn. 7}$$

$$2OH^- + Mg^{2+} \leftrightarrow Mg(OH)_2 \downarrow \tag{Rxn. 8}$$

As shown in Figure 9, the ionic activity products of magnesium hydroxide, $\log(\alpha_{Mg^{2+}}\alpha^2_{OH^-})$, for both of $-0.25+0.10$ mm and $-0.40+0.25$ mm were higher than their solubility products of -11.55.[21] Thus, the precipitation of $Mg(OH)_2$ occurred and it resulted in the decrease of Mg^{2+} concentration in the leachate. The results show that a particle size <400 μm is more likely to lead to the precipitation of $Mg(OH)_2$. Therefore, the leaching data for the particle size of $-0.25+0.10$ and $-0.40+0.25$ mm were not used in the latter investigation of the leaching kinetic models. This phenomenon also led to interesting outcome in the purity of the produced Mg-bearing products. If the reaction times were kept relatively short (<10 min) for fine particle cases, the purity of MgO produced would be maintained high while the extent of Mg extraction would also be high. But if the reaction were allowed a longer time, the overall conversion toward Mg in the solution phase and the Mg/Ca molar ratio would be negatively impacted. Thus, an optimization between reaction time and the particle size should be carefully considered for the ultimate process development.

Development of kinetic models and model validation for Mg leaching from calcined magnesite

To develop a kinetic model for the Mg leaching from calcined magnesite as a function of all the reaction parameters discussed in the previous sections, the extents of Mg extraction were calculated using Eqs. 19–21 for each dissolution scenario. As shown in Figures 10a–c, the calculated results using Eq. 20, which was derived from the reaction model limited by ash layer diffusion, yielded the best fit with the experimental data in comparison with the other two kinetic models based on fluid film diffusion (Eq. 19) and surface chemical reaction (Eq. 21). This indicates that the overall reaction rate of the leaching process of calcined magnesite in NH_4Cl solutions was limited by the diffusion of the reactants through the inert ash layer to the surface of the unreacted core.

The linear relation between $1-3(1-X_{Mg})^{2/3}+2(1-X_{Mg})$ and the reaction time were observed in Figures 10b and 11a–c. From the slopes of these straight lines, the apparent reaction rate constants of Mg leaching and the correlation coefficients were obtained and are listed in Supporting Information Table S2. Next, the Arrhenius equation (Eq. 22) was used to determine the apparent activation energy of Mg and Ca dissolution

$$k_2 = k_0 e^{-\frac{E}{RT}} \tag{22}$$

where E is the apparent activation energy and k_0 is the pre-exponential factor. Equations 23 and 24 were then derived from Eq. 22 and the resulting curves are given in Supporting Information Figure S1 for Mg and Ca extraction from calcined magnesite

$$\ln(k_2) = 6.8540 - 3726.51/T \tag{23}$$

$$\ln(k_2) = 6.0298 - 5106.20/T \tag{24}$$

For Mg extraction, a correlation coefficient of 0.9897 was obtained and the apparent activation energy for Mg dissolution from particle size of $-0.50-0.40$ mm calcined magnesite was determined to be 30.98 kJ/mol. This value is smaller than that obtained by Ranjitham and Khangaonkar[13] (43.2 kJ/mol) under the experimental conditions of particle size of $-0.075-0.065$ mm, stirring speed of 1120 min^{-1}, NH_4Cl concentration of 2.48 M, and pretreatment calcination temperature of 700°C, and solid-to-liquid ratio of 50 g/l. This difference may be due to difference in surface areas of calcined magnesite used in each study.

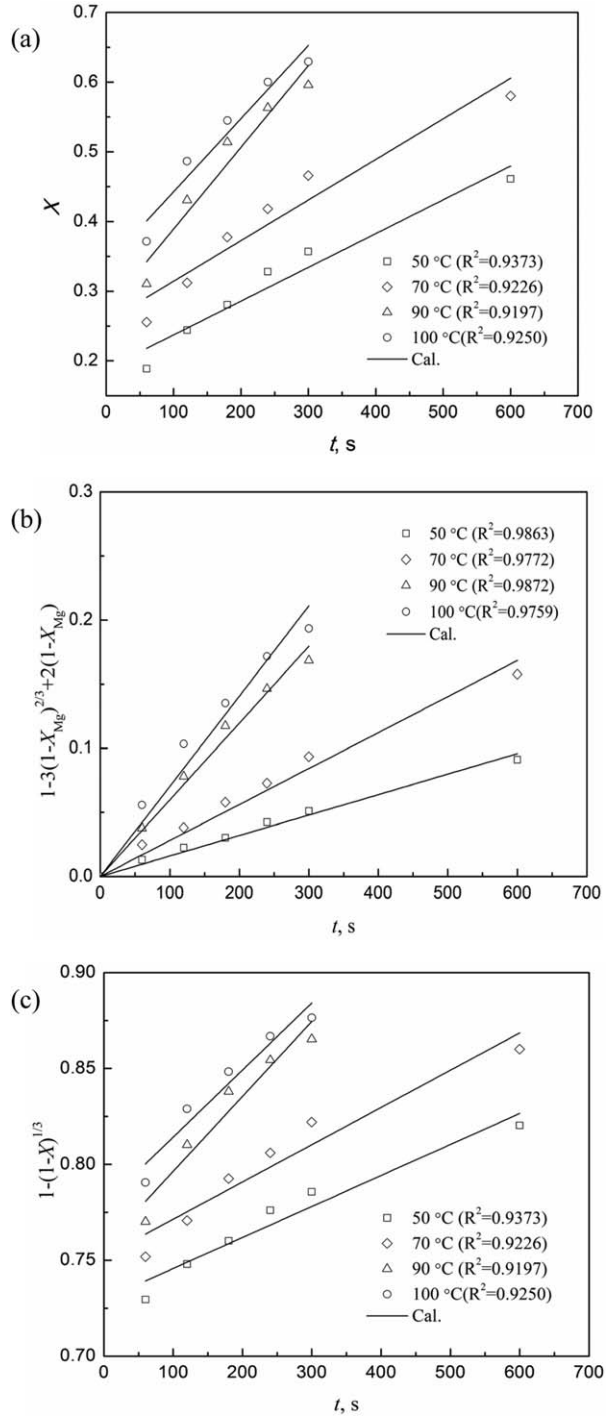

Figure 10. Variation of Mg dissolution rate with time at different reaction temperatures: (a) X, (b) $1-3(1-X)^{2/3}+2(1-X)$, (c) $1-(1-X)^{1/3}$.

The points correspond to the experimental data and the lines correspond to the predicted trends.

The apparent activation energy of Ca extraction from particle size of $-0.50-0.40$ mm was found to be 42.45 kJ/mol, which was higher than that of Mg leaching, indicating a slower reaction process. This was in agreement with the observation that at a constant leaching temperature, the Mg/Ca molar ratio decreased with increasing the reaction times (as indicated by Figure 8a-2).

To determine the effects of the reaction parameters on the rate constant, k, an empirical kinetic relationship was developed and correlated to the experimental data and it resulted in the following kinetic expression[33]

$$k_2 = k_0 C^{a1} D^{a2} (S/L)^{a3} e^{-E/RT} \tag{25}$$

where C is the concentration of NH_4Cl, D is the particle size of calcined magnesite, S/L is the solid-to-liquid ratio, and $a1$, $a2$, and $a3$ are the fitting parameters. By substituting Eq. 20 into Eq. 25, Eq. 26 was derived

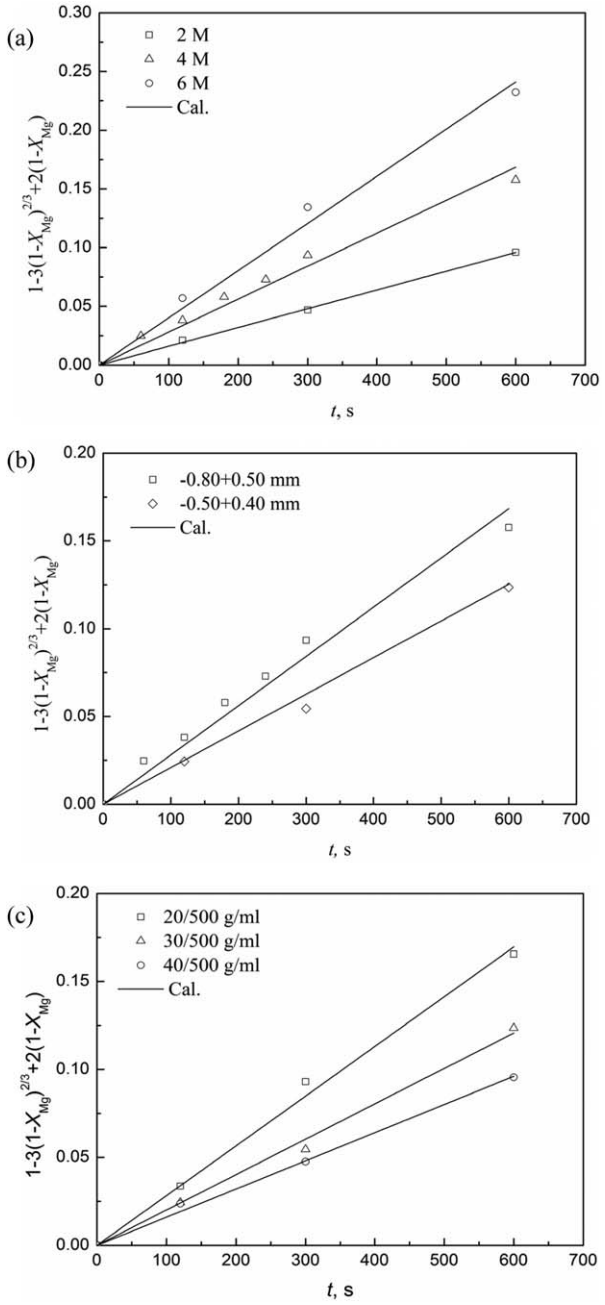

Figure 11. Variation of $1-3(1-X_{Mg})^{2/3}+2(1-X_{Mg})$ with time for different parameters: (a) NH_4Cl concentration, (b) particle size, and (c) solid-to-liquid ratio.

The points correspond to the experimental data and the lines correspond to the predicted trends.

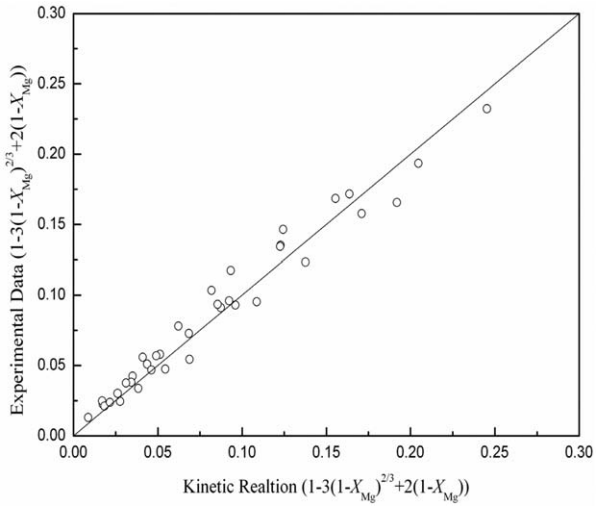

Figure 12. Comparison of kinetic relation with experimental data.

$$1\text{-}3(1\text{-}X_A)^{2/3}+2(1-X_A)=k_0C^{0.89}D^{-0.59}(S/L)^{-0.82}e^{-30980/RT}t \quad (26)$$

The parameter $a1$, $a2$, and $a3$ were determined after multiple linear regression analyses of the Mg leaching experimental data.

In Figure 12, this kinetic model was validated against the experimental data and they show good agreement with each other. The developed Mg leaching kinetic model predicts that higher concentration of NH_4Cl, smaller particle size of calcined magnesite and lower solid-to-liquid ratio will lead to greater extraction of Mg from calcined low-grade magnesite.

Leaching process with distillation of the ammonia

As we can see from the leaching kinetic data obtained above, the extraction of Mg from calcined low-grade magnesite through one leaching step was below 70%. To increase extraction of Mg and obtain higher concentration of $MgCl_2$ in the leach liquor, NH_3 in solution during the leaching process must be effectively removed. Therefore, leaching experiments by distillation of the ammonia in the leaching liquor were conducted under the calcination temperature of 650°C, NH_4Cl concentration of 6 M, initial particle size of $-0.50-0.40$ mm, and solid-to-liquid ratio of 60 g/L.

The results indicate that most of ammonia gas in solution was released, and the final concentration of Mg in the solution reached is as high as 1.18 mol/L. The conversion in terms of extracted Mg from calcined low-grade magnesite was 94.08%. However, the Mg/Ca molar ratio of <100 obtained was negatively impacted, because the reaction time lasted more than 240 min. This phenomenon is also confirmed in the section "Optimization of Reaction Parameters for High Mg to Ca Ratio". Therefore, to produce high-purity MgO with $<0.5\%$ CaO, the leaching liquor obtained by this method need one more purification step to remove extra calcium.

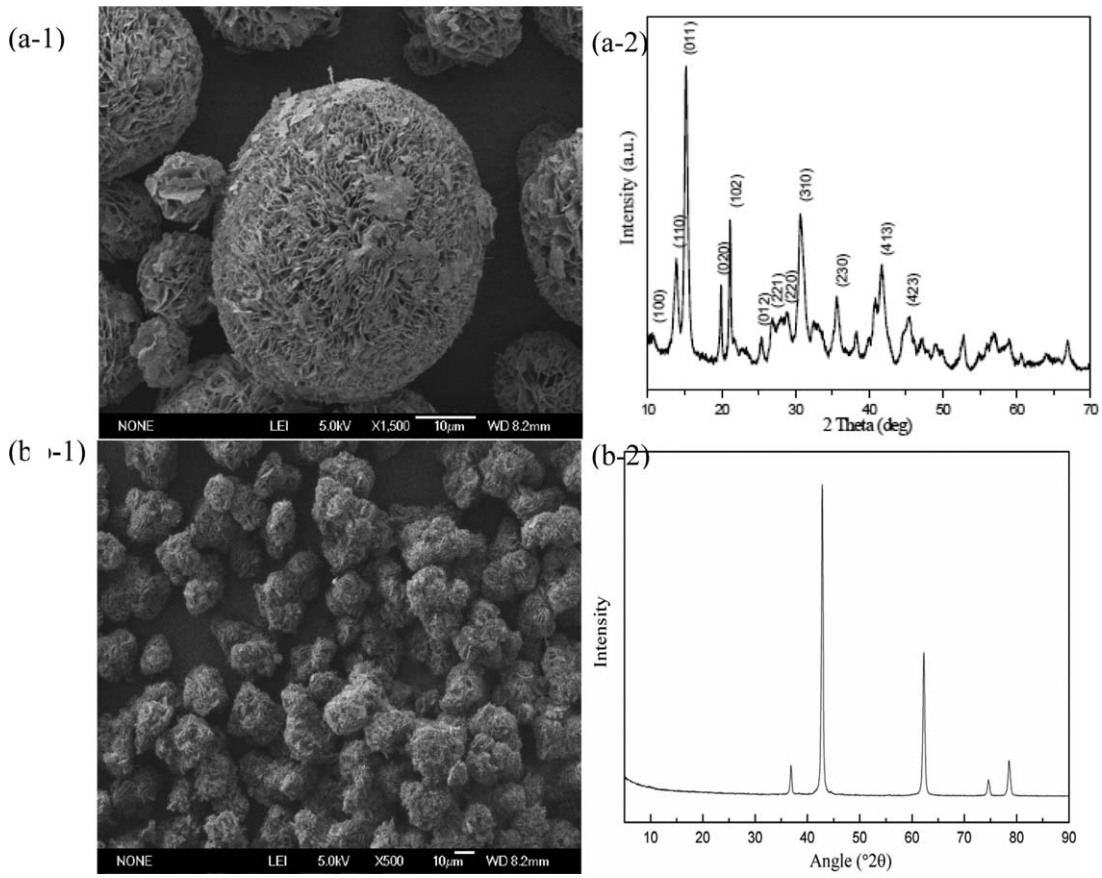

Figure 13. SEM images showing the morphologies of hydromagnesite and calcined hydromagnesite (MgO) particles: (a-1) hydromagnesite and (b-1) MgO; XRD pattern of the hydromagnesite and MgO: (a-2) hydromagnesite and (b-2) MgO.

Integration of the overall process and characterization of final MgO product

Based on the optimum leaching parameters determined throughout this study (i.e., calcination temperature of 650°C, leaching temperature of 70°C, stirring speed of 400 rpm, NH_4Cl concentration of 6 M, reaction time of 10 min, initial particle size of $-0.50-0.40$ mm, and solid-to-liquid ratio of 60 g/L), an overall process described in Figure 1 was designed and performed to produce high purity MgO. After the first leaching step (Leaching I), the extent of Mg leaching reached 67%. To enhance the overall conversion in terms of Mg extraction from calcined magnesite, the filter cake (S1) was treated again using the NH_4Cl solvent under the same experimental conditions as for the first leaching step. After the second leaching step (Leaching II), the overall conversion in terms of extracted Mg from calcined magnesite was as high as 98%. The produced magnesium chloride was in the level of 0.625 mol/L (L1) and served as intermediate for the formation of magnesium carbonate hydrate. It was obtained by mixing the two leach liquors obtained from Leaching units I and II in Figure 1. The final filter cake (S2) was comprised mainly of SiO_2 and $CaCO_3$, and it was suggested that they may be used as raw material for cement production to provide additional economic benefit.

After the leaching step, the NH_3 and CO_2 gases were introduced into the combined leach liquor to precipitate magnesium carbonate hydrate. In our previous work,[20,34] regular spherical-like particles of $4MgCO_3{\cdot}Mg(OH)_2{\cdot}4H_2O$ were successfully synthesized at reaction temperatures above 80°C. Therefore, in this study, the precipitation temperature of 80°C was selected to produce the $4MgCO_3{\cdot}Mg(OH)_2{\cdot}4H_2O$ intermediate. This intermediate was then further processed and thermally decomposed into MgO. The filtrate L2 containing NH_4Cl was then recycled to the Leaching I unit. By utilizing CO_2 from calciners and NH_3 off-gas from the Leaching I and II units in the carbonation/precipitation process, the overall chemical needs of the MgO production process were minimized.

The precipitated solid products were dried in an oven at 50°C for 10 h and SEM images of the dried hydromagnesite were obtained as well as the XRD patterns. As seen in Figure 13a-1, $4MgCO_3{\cdot}Mg(OH)_2{\cdot}4H_2O$ particles were irregular spheres resulting from interconnected thin flakes. As shown in Figure 13a-2, all diffraction peaks in the XRD patterns were indexed to be characteristic peaks of $4MgCO_3{\cdot}Mg(OH)_2{\cdot}4H_2O$ with unit cell parameters of $a = 10.11$, $b = 8.94$, and $c = 8.38$ Å and $\beta = 114.58°$ as confirmed from the reported data (JCPDS file no. 25–0513). The final product, MgO, was then obtained by thermally decomposing the dried hydromagnesite at 800°C for 4 h. The SEM images and XRD patterns of the resulting product is shown in Figures 13b-1, b-2. The data confirm the presence of the MgO crystal structure. The purity of MgO was estimated to be 99.09% and its CaO content was only limited to 0.32%.

Conclusions

A systematic kinetic and mechanistic study was conducted to determine the leaching behaviors of Mg as well as Ca from calcined low grade magensite using the NH_4Cl solvent. First, to develop a unique recycling scheme for off-gases (NH_3 and CO_2) and to fully understand the reaction kinetics with inherent pH shift, the phase equilibria of the NH_4Cl-$MgCl_2$-NH_3-H_2O systems were investigated based on the MSE model embedded in the OLI platform. This model successfully embodied the phase behavior of the leach liquor for binary cases of NH_4Cl and $MgCl_2$ dissolution in the aqueous phase. However, a new set of parameters had to be obtained for the case of the ternary systems involving NH_4Cl and $MgCl_2$. Next, the leaching kinetics, the extent of Mg extraction and the purity of produced Mg in terms of the Mg/Ca molar ratio were studied while varying the calcination temperature, dissolution temperature, NH_4Cl concentration, solid-to-liquid ratio, and particle size. The maximum conversion and highest Mg purity were achieved with the calcination temperature of 650°C, reaction temperature of 70°C, NH_4Cl concentration of 6 M, and solid-to-liquid ratio of 60 g/L. Based on the unreacted shrinking core model, three different rate-limiting cases (i.e., fluid film diffusion, ash layer diffusion, and surface reaction) were considered and it was found that the overall reaction rate was controlled by the diffusion of the reactant through the inert ash layer formed during the dissolution of calcined magnesite. An empirical kinetic equation in terms of the NH_4Cl concentration, particle size, and solid-to-liquid obtained was developed to describe the Mg leaching process from calcined magnesite in the presence of the NH_4Cl solvent. Finally, under the optimal reaction conditions determined in this study, MgO with a purity of 99.09% was obtained by optimizing the production of a leach liquor with a high Mg/Ca molar ratio. The design of the overall process involves the recycling of NH_4Cl, NH_3, and CO_2 and did not require additional purification steps for the produced MgO. Therefore, this reaction pathway could be an option for more sustainable hydrometallurgical magnesium leaching.

Acknowledgments

This work was supported by the National Natural Science Foundation of China (21206165, U1407111, 21476235, and U1407112) and the Li Foundation USA, Inc.

Notation

X_A = the extent of Mg and Ca dissolution
C_A = the concentration of Mg^{2+} or Ca^{2+} in the liquid phase ($mol{\cdot}L^{-1}$)
V = the volume of the leaching aqueous solution (L)
W = the weight of the added sample (g)
x = the mole fraction of the species
x_A = the element content of Mg or Ca in the added sample
MW_A = the molecular weight of Mg^{2+} or Ca^{2+} ($g{\cdot}mol^{-1}$)
T = the temperature (K)
$\Delta_R\bar{G}^0$ = the partial molar standard-state Gibbs free energy of the reaction ($kJ{\cdot}mol^{-1}$)
G^{ex}_{LR} = the contribution of long-range electrostatic interactions ($kJ{\cdot}mol^{-1}$)
G^{ex}_{SR} = the short-range contribution ($kJ{\cdot}mol^{-1}$)
G^{ex}_{MR} = the additional middle-range term ($kJ{\cdot}mol^{-1}$)
R = the universal gas constant ($8.314\ J{\cdot}mol^{-1}{\cdot}K^{-1}$)
K = the equilibrium constant
I_x = the ionic strength
B_{ij} = the binary interaction parameter between the species i and j
b_{ij} and c_{ij} = the adjustable parameters.
BMD# and CMD# = the interaction parameters
W_1 = the mass transfer rate of H^+ ($mol{\cdot}s^{-1}$)
W_2 = the diffusion rate of H^+ ($mol{\cdot}s^{-1}$)
W_3 = the rate of consumption of H^+ ($mol{\cdot}s^{-1}$)
C_b = the concentration of H^+ in the bulk fluid ($mol{\cdot}L^{-1}$)
C_s = the concentration of H^+ at the external surface of the particle ($mol{\cdot}L^{-1}$)

C_c = the concentration of H^+ at the surface of the un-reacted core ($mol \cdot L^{-1}$)
k_l = the mass transfer coefficient
r_0 = the radius of particle (m)
D_{eff} = the effective diffusion coefficient
k_r = the reaction rate constant
k_1, k_2, k_3 = the reaction rate constants
R_s = the main reaction rate ($mol \cdot s^{-1}$)
t = the leaching time (s)
M = the molar weight of particle ($g \cdot mol^{-1}$)
ρ_s = the particle density ($g \cdot cm^{-3}$)
E = the apparent activation energy ($J \cdot mol^{-1}$)
k_0 = the pre-exponential factor

Literature Cited

1. Kogel JE, Trivedi NC, Barker JM, Krukowski ST. Industrial Minerals and Rocks, 7th ed. Society for Mining, Metallurgy, and Exploration Inc., (U. S.) 2006.
2. Habashi F. Dissolution of minerals and hydrometallurgical processes. *Naturwissenschafter*. 1983;70:403–411.
3. Özdemir M, Çakır D, Kıpçak L. Magnesium recovery from magnesite tailings by acid leaching and production of magnesium chloride hexahydrate from leaching solution by evaporation. *Int J Miner Process*. 2009;93:209–212.
4. Kurtbas A. The heterogeneous reaction kinetics of natural magnesite with HCl. Master of Science Thesis. Ataturk University, Erzurum, Turkey, 1989.
5. Özbek H, Abali Y, Çolak S, Ceyhun I, Karagölge Z. Dissolution kinetics of magnesite mineral in water saturated by chlorine gas. *Hydrometallurgy*. 1999;51:173–185.
6. Raschman P, Fedoročková A. Study of inhibiting effect of acid concentration on the dissolution rate of magnesium oxide during the leaching of dead-burned magnesite. *Hydrometallurgy*. 2004;71:403–412.
7. Demir F, Lacin O, Dönmez B. Leaching kinetics of calcined magnesite in citric acid solution. *Ind Eng Chem Res*. 2006;45:1307–1311.
8. Lacin O, Dönmez B, Demir F. Dissolution kinetics of magnesite in acetic acid solution. *Int J Miner Process*. 2005;75:91–99.
9. Demir F, Dönmez B, Çolak S. Leaching kinetics of magnesite in citric acid solutions. *J Chem Eng Jpn*. 2003;36(6):683–688.
10. Ekmekyapa A, Erşahan H, Dönmez B. Calcination of magnesite and leaching kinetics of magnesia in aqueous carbon dioxide. *J Doga Turkish*. 1993;17:197–204.
11. Bayrak B, Laçin O, Bakan F, Saraç H. Investigation of dissolution kinetics of natural magnesite in gluconic acid solutions. *Chem Eng J*. 2006;117:109–115.
12. Bayrak B, Laçin O, Bayrak B, Saraç H. Dissolution kinetics of natural magnesite in lactic acid solutions. *Int J Miner Process*. 2006;80:27–34.
13. Ranjitham AM, Khangaonkar PR. Leaching behaviour of calcined magnesite with ammonium chloride solutions. *Hydrometallurgy*. 1990;23:177–189.
14. Raschman P. Leaching of calcined magnesite using ammonium chloride at constant pH. *Hydormetallurgy*. 2000;56:109–123.
15. Glaser V, Vidensky J, Kuzela M. Kinetics of the reaction between magnesium oxide and ammonium chloride solution. *Collect Czechoslov Chem Commun*. 1988;53:1711–1717.
16. Atashi H, Fazlollahi F, Tehrani.rad S. Leaching kinetics of calcined magnesite in ammonium chloride solutions. *Aust J Basic Appl Sci*. 2010;4:5956–5962.
17. Tzeferis PG, Agatzini-Leonardou S. Leaching of nickel and iron from greek nonsulphide nickeliferous ores by organic acids. *Hydrometallurgy*. 1994;36:345–360.
18. Ainscow WS. A new process to beneficiate magnesite to high quality sinter magnesia. *Refractories J*. 1984;59:6–13.
19. Ainscow WS, Gadgil BB. Process for producing magnesium oxide. US Patent 4,720,375. January 19, 1988.
20. Wang DG, Li ZB. Gas-liquid reactive crystallization kinetics of hydromagnesite in the $MgCl_2$-CO_2-NH_3-H_2O system: its potential in CO2 sequestration. *Ind Eng Chem Res*. 2012;51:16299–16310.
21. OLI Aqueous Electrolytes Process Chemistry, Inorganic and Organic, MSE and AQ models. Available at http://www.olisystems.com/ (accessed on June 2, 2012).
22. Tanger JC, Helgeson HC. Calculation of the thermodynamic and transport properties of aqueous species at high pressures and temperatures; revised equations of state for the standard partial molal properties of ions and electrolytes. *Am J Sci*. 1988;288:19–98.
23. Sahimi M, Gavalas GR, Tsotsis T. Statistical and continuum models of fluid-solid reactions in porous media. *Chem Eng Sci*. 1990;45:1449–1452.
24. Homma S, Ogata S, Koga J, Matsumoto S. Gas-solid reaction model for a shrinking spherical particle with unreacted shrinking core. *Chem Eng Sci*. 2005;60:4971–4980.
25. Liu B, Du H, Wang SN, Zhang Y, Zheng SL, Li LJ, Chen DH. A novel method to extract vanadium and chromium from vanadium slag using molten NaOH-$NaNO_3$ binary system. *AIChE J*. 2012;59:541–552.
26. Braun A, Bärtsch M, Schnyder B, Kötz R. A model for the film growth in samples with two moving reaction frontiers-an application and extension of the unreacted-core model. *Chem Eng Sci*. 2000;55:5273–5282.
27. Levenspiel O. Chemical Reaction Engineering, 2nd ed. New York: Wiley, 1972.
28. Rumpf B, Maurer G. Solubility of ammonia in aqueous solutions of sodium sulfate and ammonium sulfate at temperature from 333.15 K to 433.15 K and pressure up to 3 MPa. *Ind Eng Chem Res*. 1993;32:1780–1789.
29. Seidell A. Solubilities of Inorganic and Metal Organic Compounds, 3th ed. Washington, DC: American Chemical Society, 1958.
30. Ji XY, Lu XH, Zhang LZ, Bao NZ, Wang YR, Shi J, Lu Benjamin CY. A further study of solid-liquid equilibrium for the NaCl-NH_4Cl-H2O system. *Chem Eng Sci*. 2000;55:4993–5001.
31. Wang DG, Li ZB. Modeling solid-liquid equilibrium of NH_4Cl-$MgCl_2$-H_2O system and its application to recovery of NH_4Cl in MgO production. *AIChE J*. 2011;57:1595–1606.
32. Gadikota G, Swanson EJ, Zhao HJ, Park A-H. Experimental design and data analysis for accurate estimation of reaction kinetics and conversion for carbon mineralization. *Ind Eng Chem Res*. 2014;53:6664–6676.
33. Demirkiran N. A study on dissolution of ulexite in ammonium acetate solutions. *Chem Eng J*. 2008;141:180–186.
34. Wang JF, Li ZB. Crystallization and agglomeration kinetics of hydromagnesite in the reactive system $MgCl_2$-Na_2CO_3-NaOH-H_2O. *Ind Eng Chem Res*. 2012;51:7874–7883.

Manuscript received July 6, 2014, and revision received Oct. 20, 2014.